

FERMIONIC AND BOSONIC BUBBLES AND FOAM ^a

Aurel BULGAC¹, Siu A. CHIN^{2,3}, Harald A. FORBERT², Piotr MAGIERSKI^{1,4,5}
and Yongle YU¹

¹*Department of Physics, University of Washington, Seattle, WA 98195-1560, USA*

² *Department of Physics and Center for Theoretical Physics, Texas A&M University, College Station, TX 77843, USA*

³ *Institute for Nuclear Theory, University of Washington, Seattle, WA 98195-1550, USA*

⁴ *The Royal Institute of Technology, Physics Department Frescati, Frescativägen 24, S-10405, Stockholm, SWEDEN*

⁵ *Institute of Physics, Warsaw University of Technology, ul. Koszykowa 75, PL-00662, Warsaw, POLAND*

The positioning of one or more bubbles inside a many fermion or boson system, does not affect the volume, surface or curvature terms in the liquid drop expansion of the total energy. If Coulomb effects are irrelevant, the only contribution to the ground state energy of a system with one or more voids arises from quantum effects, which is similar to the Casimir effect in vacuum or in critical phenomena. We discuss the characteristics of such systems, the interplay among various effects, such as shell corrections and chaotic behavior, and briefly mention the role of the temperature and pairing.

1 Introduction

There are a number of situations when the formation of voids is favored. When a system of particles has a net charge, the Coulomb energy can be significantly lowered if a void is created. The total energy can be lowered ^{1,2}, despite an increase in surface energy. One can thus naturally expect that the appearance of bubbles will be favored in relatively heavy nuclei. This situation has been considered many times over the last 50 years in nuclear physics and lately similar ideas have been put forward for highly charged alkali metal clusters ³.

The formation of gas bubbles is another suggested mechanism which could lead to void(s) formation ⁴. The filling of a bubble with gas prevents it from collapsing. In a similar manner the air bubbles in an ordinary glass of water or steam bubbles in boiling water are stabilized. Various heterogeneous atomic

^aInvited talk given at *Collective Excitations in Fermi and Bose Systems*, September 14–17, 1998, Serra Negra, Brazil, to be published by World Scientific, eds. Carlos Bertulani and Mahir Hussein.

clusters⁵ and halo nuclei⁶ can be thought of as some kind of bubbles as well. In these cases, the Fermions reside in a rather unusual mean-field, with a very deep well near the center of the system and a very shallow and extended one at its periphery. Since the amplitude of the wave function in the semiclassical limit is proportional to the inverse square root of the local momentum, the single particle wave functions for the weakly bound states will have a small amplitude over the deep well. If the two wells have greatly different depths, the deep well will act almost like a hard wall (in most situations).

Several aspects of the physics of bubbles in Fermi and Bose systems have not been considered so far in the literature. It is tacitly assumed that a bubble position has to be determined according to symmetry considerations. For a Bose system one can easily show that a bubble has to be off-center⁷. A system of independent and noninteracting Bosons is a particularly simple system at $T = 0$, since all the particles will have the same single particle wave function. If now one would like to “drill” a hole, it would be more costly to do that in a region where the amplitude of the wave function is large, namely in the center of the system. A hole in a region where the wave function has a node should be almost “painless”. The greater the amplitude of the wave function the greater the “pain”, and thus energetically more costly. In a Bose system a hole could be created by injecting a large fullerene⁷.

In the case of a Fermi system the most favorable arrangement is not obvious and the determination of its characteristics is nontrivial⁸. The energy of a many fermion system has the general form

$$E(N) = E_{LD}(N) + E_{sc}(N) = e_v N + e_s N^{2/3} + e_c N^{1/3} + E_{sc}(N), \quad (1)$$

where E_{LD} is the smooth liquid drop part of the total energy and E_{sc} is the pure quantum shell correction contribution to the total energy. We shall consider in this work only one type of Fermions with no electric charge. In a nuclear system the Coulomb energy depends rather strongly on the actual position of the bubble. In an alkali metal cluster, as the excess charge is always localized on the surface, the Coulomb energy is essentially independent of the bubble position.

Once a bubble is formed, its position does not affect the volume, surface or curvature terms in the liquid drop mass formula. Only quantum effects are left responsible for determining the optimal geometrical configuration. The character of the shell corrections is strongly correlated with the existence of regular and/or chaotic motion¹⁰. If a spherical bubble appears in a spherical system and if the bubble is positioned at the center, then for certain “magic” Fermion numbers the shell correction energy E_{sc} , and hence the total energy $E(N)$, has a very deep minimum. However, if the number of particles is not

“magic”, in order to become more stable the system will in general tend to deform. Real deformations lead to an increased surface area and liquid drop energy. On the other hand, merely shifting a bubble off-center deforms neither the bubble nor the external surface and therefore, the liquid drop part of the total energy of the system remains unchanged.

Moving the bubble off-center can often lead to a greater stability of the system due to shell correction energy effects. In large systems the relative importance of the shell correction energy E_{sc} is small – it increases with N at a rate even smaller than the curvature energy.

In recent years it was shown however that in a 2-dimensional annular billiard, i.e. in the 2-dimensional analog of spherical bubble nuclei, the motion becomes more chaotic as the bubble is moved further from the center⁹. This effect is expected to diminish the importance of the shell corrections and thus raise again, the question of whether displacing the bubble off-center can lead to more stable configurations.

One can anticipate that the relative role of various periodic orbits (diameter, triangle, square etc.) is modified in unusual ways in systems with bubbles. In 3-dimensional systems the triangle and square orbits determine the main shell structure and produce the beautiful supershell phenomenon^{10,11}. A small bubble near the center will affect only diameter orbits. After being displaced sufficiently far from the center, the bubble will first touch and destroy the triangle orbits. In a 3-dimensional system only a smaller fraction of these orbits will be destroyed. Thus one expects that the existence of supershells will not be critically affected, but that the supershell minimum will be less pronounced. A larger bubble will simultaneously affect triangular and square orbits, and thus can have a dramatic impact on both shell and supershell structure.

It is natural to consider also the formation of two or more bubbles at the same time, in finite, infinite or semi-infinite systems. For a sufficiently large bubble density a new form of matter can be created, foam. One might argue that sometimes a “misty” state could be more likely. As in the case of percolation, whether a “foamy” or a “misty” state would be formed, should strongly depend on the average matter density. At very low average densities, formation of droplets is more likely, while at higher average densities (lower than the equilibrium density however) the formation of a foam is more probable. Similar ideas have been explored for the case of neutron matter and various “exotic” structures have been found, such as bubbles, plates/lasagna, and rods/spaghetti¹². The energetics of two or more bubbles, their relative placements and positions with respect to boundaries, their collisions and bound state formation, their impact on the role played by periodic or chaotic trajectories, and their temperature dependence, are but a few in a long list of challenging questions.

A plethora of new, extremely soft collective modes is thus generated. The character of the response of such systems to various external fields is an extremely intricate issue. Since the energy of the system changes only very little while the bubble(s) is being moved, a slight change in energy can result in large scale bubble motion. Such a system may prove to be an extremely sensitive “detector”.

In Section 2 we describe two numerical methods we have developed in order to determine the single-particle spectrum of quantum billiards. In Section 3 we describe the case of one bubble in a spherical system, in Section 4 the case of two bubbles in an infinite medium and we conclude with several final remarks in the last Section.

2 Methods to determine the single-particle spectrum for quantum billiards of arbitrary shapes

The change of the total energy of a many Fermion system can be computed quite accurately using the shell corrections method, once the single-particle spectrum is known as a functions of the shape of the system¹³. We describe here briefly two methods we have developed in order to determine the eigenvalue spectrum of quantum billiards of arbitrary shapes: the conformal mapping method and the boundary overlap method (BOM). The methods known in literatures are suited to so called star shaped domains¹⁴ and they meet with significant and/or unsurmountable difficulties when the domains of interest have unusual topologies and/or shapes.

2.1 Conformal mapping of the eigenvalue problem

This method is especially suited for treating systems with round bubbles. By means of an appropriately chosen conformal transformation, a single-connected 2-dimensional region can be transformed into a circular annulus. We shall consider here three different cases: *i*) a circular hole inside a circular cavity; *ii*) two circular holes in an infinite medium, and *iii*) a hole in a semi-infinite medium.

Even though the partial differential equation is the same:

$$-[\partial_u^2 + \partial_v^2]\Psi(u, v) = k^2\Psi(u, v), \quad (2)$$

the Dirichlet boundary conditions in the first two cases are imposed on the following two circles

$$\Psi(u, v)|_{\mathcal{B}} = 0 \quad \text{where} \quad \mathcal{B} = \{u^2 + v^2 = R^2 = 1 \cup (u - d)^2 + v^2 = a^2\}, \quad (3)$$

(we have chosen here a coordinate scale such that $R = 1$) $0 \leq a \leq R$, $0 \leq d \leq R = 1$ and $0 \leq a + d \leq R = 1$ in the first case and $0 \leq a$ and $a + R = a + 1 \leq d$ in the second case. By means of the conformal transformation

$$w = \frac{z - c}{1 - zc}, \quad w = u + iv, \quad z = x + iy \quad (4)$$

$$c = \frac{1 + d^2 - a^2 - \sqrt{(1 + d^2 - a^2)^2 - 4d^2}}{2d} \quad (5)$$

the unit circle $u^2 + v^2 = R^2 = 1$ is mapped onto itself, while the circle $(u - d)^2 + v^2 = a^2$ becomes a concentric circle with a radius:

$$r = \left| \frac{d + a - c}{1 - c(d + a)} \right| \quad (6)$$

with $r < 1$ in the first case and $r > 1$ in the second case. The third case, when the boundary is

$$\mathcal{B} = \{(u + d)^2 + v^2 = a^2 \cup \operatorname{Re} z = u = 0\} \quad (7)$$

can be handled with a similar conformal transformation, namely

$$w = \frac{A + 1}{A - 1} \frac{z + A(d + a)}{z - A(d + a)}, \quad A = \sqrt{\frac{d - a}{d + a}}. \quad (8)$$

Under this transformation the circle in the left plane (by convention $d > 0$) becomes the unit circle with the center at the origin, while the imaginary axis becomes a concentric circle of radius

$$r = \frac{1 + A}{1 - A} \geq 1. \quad (9)$$

The partial differential equation then becomes

$$-J(x, y)[\partial_x^2 + \partial_y^2]\Psi(x, y) = k^2\Psi(x, y), \quad (10)$$

where $x = \rho \cos \phi$, $y = \rho \sin \phi$ and where for the first two geometries

$$J(x, y) = \left| \frac{\partial z}{\partial w} \right|^2 = \frac{[(1 - cx)^2 + c^2y^2]^2}{(1 - c^2)^2} = \frac{[1 + c^2\rho^2 - 2c\rho \cos \phi]^2}{(1 - c^2)^2} \quad (11)$$

and

$$J(x, y) = \frac{(1 + A)^2[(x - A)^2 + y^2]^2}{4A^2(1 - A)^2} = \frac{(1 + A)^2[\rho^2 + A^2 - 2A\rho \cos \phi]^2}{4A^2(1 - A)^2} \quad (12)$$

in the case of the third geometry.

One can now expand the eigenfunction $\Psi(x, y)$ in the complete set of states of the on-center problem with $J(x, y) = 1$,

$$\Phi_{n,m}(\rho, \phi) = C_n [J_m(p_n \rho) Y_m(p_n r) - Y_m(p_n \rho) J_m(p_n r)] \exp(im\phi), \quad (13)$$

$$[J_m(p_n R) Y_m(p_n r) - Y_m(p_n R) J_m(p_n r)] = 0, \quad (14)$$

$$\langle \Phi_{nm} | \Phi_{n'm'} \rangle = \delta_{nn'} \delta_{mm'} \quad (15)$$

where m is the magnetic quantum number, $J_m(x)$ and $Y_m(x)$ are the cylindrical Bessel functions of the first and second kind, C_n is a normalization constant, p_n^2 are the corresponding eigenvalues of the on-center problem. Using the following representation of the eigenfunction $\Psi(\rho, \phi)$

$$\Psi(\rho, \phi) = \sum_{nm} A_{nm} \frac{1}{k_n} \Phi_{n,m}(\rho, \phi) \quad (16)$$

one can easily establish that the expansion coefficients A_{nm} for the eigenfunctions and the eigenvalues of the off-center problem can be determined from the following eigenvalue problem

$$\sum_{n'm'} k_n \langle \Phi_{nm} | J | \Phi_{n'm'} \rangle k_{n'} A_{n'm'} = k^2 A_{nm}. \quad (17)$$

This matrix is block-diagonal as the matrix elements $\langle \Phi_{nm} | J | \Phi_{n'm'} \rangle$ vanish for $|m - m'| > 2$.

The 3-dimensional case, when circles become spheres and lines become planes, can be easily treated in a similar manner. For all the geometries corresponding to the 2-dimensional cases described above the problem has an axial symmetry, corresponding to a simple reflection symmetry $y \rightarrow -y$ in the 2-dimensional problem. It is easy to show that the eigenfunctions have the following form

$$\Psi(\rho, \phi, z) = \frac{\psi_m(\rho, z) \exp(im\phi)}{\sqrt{\rho}} \quad (18)$$

where $\Psi(\rho, z)$ satisfy the partial differential equation

$$\left[-(\partial_\rho^2 + \partial_z^2) + \left(m^2 - \frac{1}{4} \right) \frac{1}{\rho^2} \right] \psi_m(\rho, z) = k^2 \psi_m(\rho, z), \quad (19)$$

with the obvious boundary condition $\psi(\rho = 0, z) = 0$. By performing similar conformal transformations in the upper half-complex plane $z + i\rho$, one can reduce the 3-dimensional problems to one similar to the 2-dimensional cases discussed above.

2.2 Boundary overlap method

The solution of the Helmholtz equation for the 2-dimensional annular billiard can be represented as follows

$$\Psi(u, v) = \sum_m C_m \Phi_m(k\rho, \phi), \quad (20)$$

$$\Phi_m(k\rho, \phi) = [J_m(k\rho)Y_m(ka) - J_m(ka)Y_m(k\rho)] \exp(im\phi), \quad (21)$$

with the yet undetermined coefficients C_m . Obviously, this basis set is not unique, but it is the best suited one for the problem at hand⁸. By requiring that the boundary overlap vanishes

$$\frac{1}{2\pi R} \oint_{\mathcal{B}} dl \sum_{m_1, m_2} C_{m_1}^* \Phi_{m_1}^*(k_0\rho, \phi) \Phi_{m_2}(k_0\rho, \phi) C_{m_2} \quad (22)$$

$$= \sum_{m_1, m_2} C_{m_1}^* \mathcal{O}_{m_1, m_2}(k_0) C_{m_2} = 0 \quad (23)$$

one can determine the eigenvalues and the eigenvectors. This quantization condition is satisfied only for discrete values of k_0 . For arbitrary values of k one can introduce the eigenvalues and eigenvectors of the boundary overlap matrix (BOM) $\mathcal{O}(k)$

$$\mathcal{O}(k)C_\alpha = \lambda_\alpha(k)C_\alpha. \quad (24)$$

From the non-negativity of the boundary norm it follows that for real values of k these eigenvalues satisfy the inequality $\lambda_\alpha(k) \geq 0$ and only for an eigenvalue of our initial problem $\lambda_\alpha(k_0) = 0$. In the neighborhood of such an eigenvalue $\lambda_\alpha(k) \propto (k - k_0)^2 + \dots$. The basic idea behind our approach is to analytically continue BOM $\mathcal{O}(k)$ into the complex k -plane and to compute around a contour \mathcal{C} the integral

$$\mathcal{N}(\mathcal{C}) = \oint_{\mathcal{C}} \frac{dk}{4\pi i} \sum_\alpha \frac{\lambda'_\alpha(k)}{\lambda_\alpha(k)}, \quad (25)$$

where $\lambda'_\alpha(k)$ is the derivative of the eigenvalue $\lambda_\alpha(k)$ with respect to k , which can be evaluated using the simple formula

$$\lambda'_\alpha(k) = C_\alpha^\dagger(k) \mathcal{O}'(k) C_\alpha(k). \quad (26)$$

Above, $\mathcal{O}'(k)$ is the derivative of $\mathcal{O}(k)$ with respect to k and the eigenvectors are normalized as usual, $C_\alpha^\dagger(k)C_\alpha(k) = 1$ (vector and matrix multiplication rules are implied in previous formulae). Thus $\mathcal{N}(\mathcal{C})$ is equal to the number

of eigenvalues (counting the degeneracies as well) located on the segment of the real k -axis enclosed by the contour \mathcal{C} . Using a similar formula one can compute the energy of an \mathbf{N} -Fermion system

$$E_{\mathbf{N}} = \oint_{\mathcal{C}} \frac{dk}{4\pi i} \sum_{\alpha} \frac{\lambda'_{\alpha}(k)}{\lambda_{\alpha}(k)} k^2, \quad (27)$$

where the number of Fermions is given by

$$\mathbf{N} = \mathcal{N}(\mathcal{C}). \quad (28)$$

We shall not dwell here on various numerical subtleties, as the issues regarding the numerical implementation of the BOM method will be described in more detail elsewhere⁸.

3 One bubble in a finite system

The simplest case to consider is a circular 2-dimensional Fermi or Bose system, in which one can “drill” a circular hole and determine how the ground state energy of the system changes when the hole is displaced from the center towards the edge of the system.

In Fig. 1 we show the unfolded single-particle spectrum for the case of a bubble of half the radius of the system, $a = R/2$, as a function of the displacement d of the bubble from the center. The unfolded single-particle spectrum is determined from the Weyl formula¹⁵ for the average cumulative number of states (for spinless particles) with energy less than k^2 as follows

$$N_0(k) = \frac{S}{4\pi} k^2 - \frac{L}{4\pi} k + \frac{1}{12\pi} \oint_{\mathcal{B}} dl \kappa(l) = \frac{R^2 - a^2}{4} k^2 - \frac{R + a}{2} k, \quad (29)$$

$$e_n = N_0(k_n). \quad (30)$$

In the above formula, S is the area of the 2-dimensional system, L is its perimeter, $\kappa(l)$ is the local average curvature along the perimeter and l is the length coordinate, thus $L = \oint_{\mathcal{B}} dl$, and k_n^2 is the actual n -th energy eigenvalue. By construction the unfolded spectrum e_n has an unit average level density. When the bubble is at the center, the problem is rotationally symmetric with a highly (quasi)degenerate single-particle spectrum. The existence of symmetries, which give rises to high degeneracies in the single particle spectrum, is the basic reason for the existence of “magic numbers” and extra stable nuclei and atoms. If one were to construct a nearest-neighbor level splitting distribution, a distribution very different from the Wigner surmise should emerge in this case (we shall not display it here, however). Typically for integrable systems

the nearest-neighbor level splitting distributions have a Poissonian character. As the bubble is moved off center, the classical problem becomes more chaotic⁹. One can expect that the single particle spectrum would approach that of a random Hamiltonian¹⁶ and that the nearest-neighbor splitting distribution would be given by the Wigner surmise¹⁷. The spectrum for chaotic systems is typically very “rigid”, it shows a relatively low level of fluctuations among distant level. This particular and remarkable property of the spectrum is best illustrated by evaluating the so called Δ_3 statistics¹⁷. The Δ_3 statistics is the most reliable quantity used to establish whether a given quantum spectrum is regular or chaotic, depending on whether this statistic is closer to the Poisson or to the GOE/GUE/GSE limits (here GOE/GUE/GSE represent one of the universal Gaussian ensembles of random Hamiltonians¹⁷). A random Hamiltonian would imply that “magic” particle numbers are as a rule absent. There is a large number of level crossings in Fig. 1, but in spite of that one can definitely see a significant number of relatively large gaps in the spectrum. If the particle number is such that the Fermi level is at a relatively large gap, one can expect that the system at the corresponding “deformation” is very stable. This situation is very similar to the celebrated Jahn-Teller effect in molecules. A simple inspection of Fig. 1 suggests that for various particle numbers the energetically most favorable configuration can either have the bubble on- or off-center. Consequently, a “magic” particle number could correspond to a “deformed” system. In this respect this situation is a bit surprising, but not unique. It is well known that many nuclei prefer to be deformed, and there are particularly stable deformed “magic” nuclei or clusters^{13,21,22}.

For a (noninteracting) many Boson system only the lowest single particle level would be relevant. As it was shown by two of us⁷, it is energetically favorable to expel the bubble, as it is more costly to “drill” a hole in the center, where the single-particle wave function has a maximum, than at the edge of the system.

The variation of the ground state energy of an interacting N -Fermion system, with respect to shape deformation or other parameters, is accurately given by the shell correction energy¹³

$$\delta E(N) = \sum_{n=1}^N k_n^2 - \int_0^{k_0} dk \frac{N_0(k)}{dk} k^2, \quad (31)$$

$$N = N_0(k_0). \quad (32)$$

In our case, the eigenspectrum and the shell correction energy are functions of N , R , a and d . When the particle number N is varied at constant density, we have $R = R_0 N^{1/2}$ and $a = a_0 N^{1/2}$ in 2-D and $R = R_0 N^{1/3}$ and $a = a_0 N^{1/3}$

in 3–D. There is a striking formal analogy between the energy shell correction formula and the recipe for extracting the renormalized vacuum Casimir energy in quantum field theory¹⁸ or the critical Casimir energy in a binary liquid mixture near the critical demixing point¹⁹. In computing the shell correction energy the “trivial” liquid drop or the macroscopic dependency of the total energy, see Eq. 1, on the geometry of the system cancels out and only the pure quantum effects remain. In the $N \rightarrow \infty$ limit the shell correction energy becomes irrelevant. For a very large 3–dimensional Fermionic systems, it was shown by Strutinsky and Magner²⁰ that $\delta E(N) \propto N^{1/6}$, which is significantly less than even the curvature corrections, which behave as $\propto N^{1/3}$. In 2–dimensions the curvature term in the energy is N –independent. In Fig. 2 we show the contour plot of the shell correction energy for the same system with the (unfolded) single–particle spectrum shown in Fig. 1 ($a = R/2$) as a function of the bubble displacement d versus $N^{1/2}$. The overall regularity of “mountain ridges” and “canyons” is at least somewhat unexpected. One can see that various mountain tops and valleys form an alternating network almost orthogonal to the “mountain ridges” and “troughs”. For some N ’s the bubble “prefers” to be in the center, while for other values that is the worst energy configuration. For a given particle number N the energy is an oscillating function of the displacement d and many configurations at different d value have similar energies.

A bubble with a radius $a = R/2$ is quite large and when it is at the center, it is tangent to all classical triangular orbits. When the bubble is displaced off center one naturally expect that there are no remnants of these orbits and therefore no supershell phenomenon in this two dimensional system. It is therefore surprising that even for relatively large displacements the contour plot of the shell correction energy retained significant structure, somewhat at odds with the naive expectation that the role of triangular and square orbits should be suppressed.

What is changed if the bubble has a smaller radius? In Fig. 3 we show the unfolded single–particle spectra for a bubble with $a = R/5$. When compared to the spectra in Fig. 1 one can see that the number of level crossing is significantly smaller. One can also show that in the limit of a vanishing bubble radius “nothing happens”, see e.g. Ref. 7. As a result, the shell correction energy contour plot has less structure. This is shown in Fig. 4. The amplitude of the fluctuations are now smaller and the energy changes less in the d –direction. Thus a system with a smaller bubble is significantly softer.

Simply for the lack of space we shall not present here any results for the 3–dimensional case. It suffices to mention that the overall qualitative picture is similar to the 2–dimensional case.

4 Two identical bubbles in an infinite medium

By applying similar techniques one can study the case of two identical bubbles in an infinite medium (or a single bubble near the boundary of a semi-infinite medium). The analysis we have performed in this case is less complete. Although the single-particle spectrum is continuous, our discretization procedure produces only a discrete spectrum. We can show however, that the “wave functions” so determined are localized mostly between the two bubbles. The rest of the wave functions, which we do not determine, are in some sense “far away”, and are not very sensitive to the relative positions of the two bubbles. Increasing the size of the numerical basis set leads to a denser eigenvalue spectrum, but the dependence of the single-particle eigenvalues on the separation between the two bubbles remains unchanged. We have verified this by performing calculations with increasingly larger basis sets, up to four thousand basis states. In Fig. 5 we display the energy eigenvalues multiplied with d^α , i.e. $k_n^2(d)d^\alpha$, where d is the minimum distance between the two bubble surfaces. As one can see, for relatively small, but not too small separations, the single-particle spectrum can be fairly described by a simple power law, $k_n^2(d) \propto \varepsilon_n(d)/d^\alpha$, where $\varepsilon_n(d)$ is a slowly varying function of d and $\alpha \approx 2/5$. This naturally implies that the total energy of such a system has a similar distance dependence and thus two bubble in an infinite medium will repel each other with a simple power law potential $U(d) \propto d^{-\alpha}$. This result has a limited range of validity and cannot be expected to be correct at larger separations. At large distances one can show that the bubble–bubble interaction is similar to the Ruderman–Kittel interaction in condensed matter physics, i.e. an oscillatory potential whose amplitude decreases as a power law. When the bubble–bubble separation is much larger than the bubble radii and the Fermi wavelength one can estimate the bubble–bubble interaction using the linear response theory. Let us first assume that the two bubbles can be described as two small impurities separated by a distance \mathbf{d} . The interaction energy is given by

$$E_{12}(\mathbf{d}) = \int d\mathbf{r}_1 \int d\mathbf{r}_2 V_1(\mathbf{r}_1) \chi(\mathbf{r}_1 - \mathbf{r}_2 - \mathbf{d}) V_2(\mathbf{r}_2), \quad (33)$$

where $\chi(\mathbf{r}_1 - \mathbf{r}_2 - \mathbf{d})$ is the static form factor or the Lindhard response function of a homogeneous Fermi gas and $V_1(\mathbf{r}_1)$ and $V_2(\mathbf{r}_2)$ are the potentials describing the interaction of these two impurities with the Fermion background. Since the bubbles cannot be considered as weak impurities the potentials should be replaced by the corresponding scattering amplitudes, namely

$$T_{1,2} = V_{1,2} + V_{1,2} G T_{1,2}, \quad (34)$$

where G is the single-particle propagator. The formula for the energy shift becomes somewhat more complicated, however, the dependence on the bubble-bubble separation is not drastically modified. The asymptotic behavior is

$$E_{12}(\mathbf{d}) \propto \frac{\cos(2k_F d)}{d^3}, \quad (35)$$

where k_F is the Fermi momentum. At very small separations on the other hand, as our numerical result seem to imply, the repulsion could become stronger than a simple $\propto d^{-\alpha}$ potential, where α was determined above, see Fig. 5. When two bubbles are at a relative distance much smaller than the bubble radii, one can replace the two bubbles with two infinite parallel plates. It is straightforward to show that the interaction energy in this case is a repulsive power law potential $U(d) \propto d^{-\alpha}$, where $\alpha = 2$ or $\alpha = 1$ depending on whether the particle number or the particle density is kept constant while the distance between the plates is varied. This result thus supports qualitatively the above inference.

The short distance repulsion will prevent two bubbles from collapsing into a single bigger bubble, even though this will lower the surface energy. One could expect however the formation of “bubble molecules” of various sizes.

5 Conclusions

We did not have here the space to discuss in any detail the influence of temperature. Naively since one expects rising temperature to smooth out shell effects, the same should happen to systems with bubbles. Thus at finite temperature, the relative position of a bubble inside a many-body system or the relative positioning of two bubbles in an infinite medium, should be almost insensitive to the bubble-bubble separation. What is wrong with this type of argument however is the fact that at finite temperatures one should instead consider the free energy. The entropy of the system increases as one displaces the bubble off-center, due to a contribution, which can be called positional entropy, $S(\mathbf{d}) = \ln d + \text{const}$. Moreover, making more bubbles could lead to a further decrease of the free energy, even though the energy might increase. Thus the problem of one or more bubbles at finite temperatures has its own special intricacies.

Pairing correlations can lead to a further softening of the potential energy surface of a system with one or more bubbles. We have seen the energy of a system with a single bubble is an oscillating function of the bubble displacement. When the energy of the system as a function of this displacement has a minimum, the Fermi level is in a relatively large gap where the single-particle

level density is very low. When the energy has a maximum, just the opposite is true. On the other hand pairing correlations will be significant when the Fermi level occurs in a region of high single-particle level density. It is thus natural to expect that the total energy is lowered by paring correlations at “mountain tops”, and be less affected at “deep valleys”, which ultimately leads to further leveling of the potential energy surface.

We also did not study other types of boundary conditions, Neumann or mixed boundary conditions, at the bubble boundary and/or at the system boundary. Depending on the nature of the bubble, it may be necessary to consider these cases in the future. The change in boundary conditions can lead to completely different conclusions in specific situations.

We can make a somewhat weaker argument for why only consider spherical bubbles. In the process of deforming a bubble the surface energy changes. However, for very large particle numbers the shell correction energy is parametrically much smaller than the surface energy. Thus, at least for large systems, spherical bubbles should be energetically favored (if the surface tension is positive).

A system with one or more bubbles should be a very soft system. The energy to move a bubble is parametrically much smaller than any other collective mode. For this reasons, once a system with bubbles is formed, it could serve as an extremely sensitive “measuring device”, because a weak external field can then easily perturb the bubble(s) and produce a system with a completely different geometry. In Ref. 7 a Bose–Einstein condensate detector was suggested, which however is a detector of a slightly different nature than the one we are suggesting here. There the Bose character of the particles lead to an enhancement of the interaction between the bubble and the condensate.

There are many systems where one can expect that the formation of bubbles is possible. Known nuclei are certainly too small and it is difficult at this time to envision a way to create nuclei as big as those predicted in Ref. 2. On the other hand voids can be easily conceived to exist in neutron stars¹². Metallic clusters with bubbles are much easier to imagine. Another realistic system to consider is two or more fullerenes in either liquid sodium or liquid mercury. In the case of sodium the electron wave functions have a node at the fullerene surface while in the case of mercury they do not. Since fullerenes do not melt easily, one can also consider other liquid metals. There is another experiment that one can suggest, to place a metallic ball inside a superconducting microwave resonator of the type studied in Ref. 23 and study the ball energetics and maybe even dynamics.

Acknowledgments

AB thanks B.Z. Spivak for discussions concerning the impurity–impurity interaction, D. Tománek for suggesting a possible experiment with two fullerenes in a liquid metal, C.H. Lewenkopf for several literature leads concerning existing numerical methods for quantum billiards and G.F. Bertsch for suggesting a simple 1-dimensional “billiard” to test our methods. SAC would like to thank the Institute for Nuclear Theory at the University of Washington for hospitality during the Atomic Clusters Program, Summer, 1998. PM thanks the Nuclear Theory Group in the Department of Physics at the University of Washington for hosting his stay. AB and YY acknowledge the DOE financial support and SAC and HAF acknowledge NSF financial support.

References

1. H.A. Wilson, Phys. Rev. **69**, 538 (1946); J.A. Wheeler, unpublished notes; P.J. Siemens and H.A. Bethe, Phys. Rev. Lett. **18**, 704 (1967); C.Y. Wong, Ann. Phys. **77**, 279 (1973).
2. K. Pomorski and K. Dietrich, Nucl. Phys. **A 627**, 175(1997); Phys. Rev. Lett. **80**, 37 (1998).
3. K. Pomorski and K. Dietrich, cond-mat/9711136.
4. L.G. Moretto, K. Tso and G.J. Wozniak, Phys. Rev. Lett. **78**, 824 (1997).
5. S. Saito and F. Yabe, to be published in *Chemistry and Physics of Fullerenes and Related Materials*, vol. **6**, eds. K.M. Kadish and R.S. Ruoff, Pennington, 1998; T.P. Martin, N. Malinowski, U. Zimmermann, U. Näher, and H. Schaber, J. Chem. Phys. **99**, 4210 (1993); U. Zimmermann, N. Malinowski, U. Näher, S. Frank and T.P. Martin, Phys. Rev. Lett. **72**, 3542 (1994).
6. S.M. Austin and G.F. Bertsch, Scientific American, **272**, 62 (1995).
7. S.A. Chin and H.A. Forbert, Los Alamos e–preprint archive, cond–mat/9810269.
8. A. Bulgac and P. Magierski, in preparation.
9. O. Bohigas, S. Tomsovic and D. Ullmo, Phys. Rep. **223**, 43 (1993); O. Bohigas, D. Boosé, R. Egydio de Carvalho, and V. Marvulle, Nucl. Phys. A **560**, 197 (1993); S. Tomsovic and D. Ullmo, Phys. Rev. E **50**, 145 (1994); S.D. Frischat and E. Doron, Phys. Rev. E **57**, 1421 (1998).
10. R. Balian and C. Bloch, Ann. Phys. **67**, 229 (1972).
11. H. Nishioka, K. Hansen and B.R. Mottelson, Phys. Rev. B **42**, 9377 (1990); J. Pedersen, S. Bjornholm, J. Borggreen, K. Hansen, T.P. Martin and H.D. Rasmussen, Nature **353**, 733 (1991).

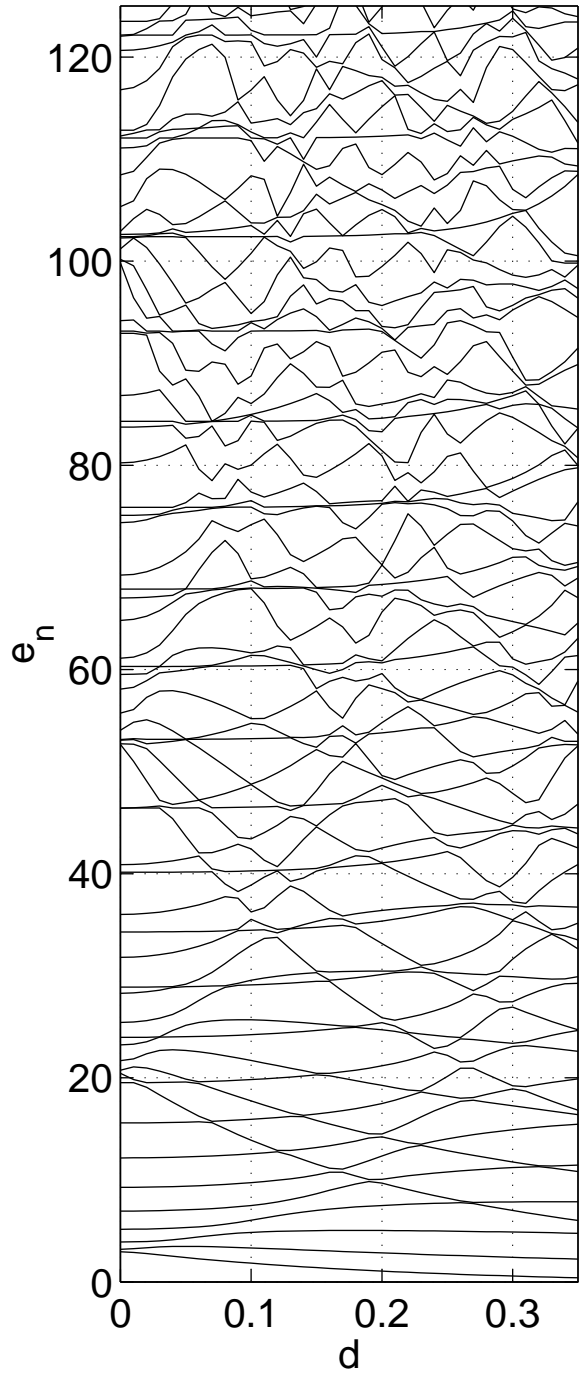
12. G. Baym, H.A. Bethe and C.J. Pethick, Nucl. Phys. **A175**, 225 (1971); C.P. Lorentz, D.G. Ravenhall and C.J. Pethick, Phys. Rev. Lett. **70**, 379 (1993); C.J. Pethick and D.G. Ravenhall, Ann. Rev. Nucl. Part. Sci. **45**, 429 (1995) and many more references therein.
13. V.M. Strutinsky, Sov. J. Nucl. Phys. **3**, 449 (1966); Nucl. Phys. **A 95**, 420 (1967); *ibid* **A 122**, 1 (1968); M. Brack, J. Damgaard, A. Jensen, H. Pauli, V. Strutinsky and C. Wong, Rev. Mod. Phys. **44**, 320 (1972); H. Nishioka, K. Hansen and B. Mottelson, Phys. Rev. **B 42**, 9377 (1990); M. Brack, *ibid* **65**, 677 (1993) and many references therein.
14. E. Vergini and M. Saraceno, Phys. Rev. E **52**, 2204–2207 (1995).
15. R.T. Waechter, Proc. Camb. Phil. Soc. **72**, 439 (1972); H.P. Baltes and E.R. Hilf, *Spectra of Finite Systems*, Wissenschaftsverlag, Mannheim, Wien, Zürich: Bibliographisches Institut, 1976.
16. O. Bohigas, M.J. Giannoni and C. Schmit, Phys. Rev. Lett. **52**, 1 (1984).
17. M.L. Mehta, *Random Matrices*, Academic Press Inc., Boston, 1991.
18. H.B.G. Casimir, Proc. K. Ned. Akad. Wet. **51**, 793 (1948); V.M. Mostepanenko and N.N. Trunov, Sov. Phys. Usp. **31**, 965 (1988) and references therein.
19. M.E. Fisher and P.G. de Gennes, C.R. Acad. Sci. Ser. B **287**, 207 (1978); A. Hanke, F. Schlesener, E. Eisenriegler and S. Dietrich, Phys. Rev. Lett. **81**, 1885 (1998) and references therein.
20. V.M. Strutinsky and A. G. Magner, Sov. J. Part. Nucl. Phys. **7**, 138 (1976).
21. A. Bohr and B. Mottelson, *Nuclear Structure*, vol. II, Benjamin, New York, (1974).
22. A. Bulgac and C. Lewenkopf, Phys. Rev. Lett. **71**, 4130 (1993).
23. H.D. Graf, H.L. Harney, H. Lengeler, C.H. Lewenkopf, C. Rangacharyulu, A. Richter, P. Schardt, H.A. Weidenmüller, Phys. Rev. Lett. **69**, 1296 (1992).

Figure captions

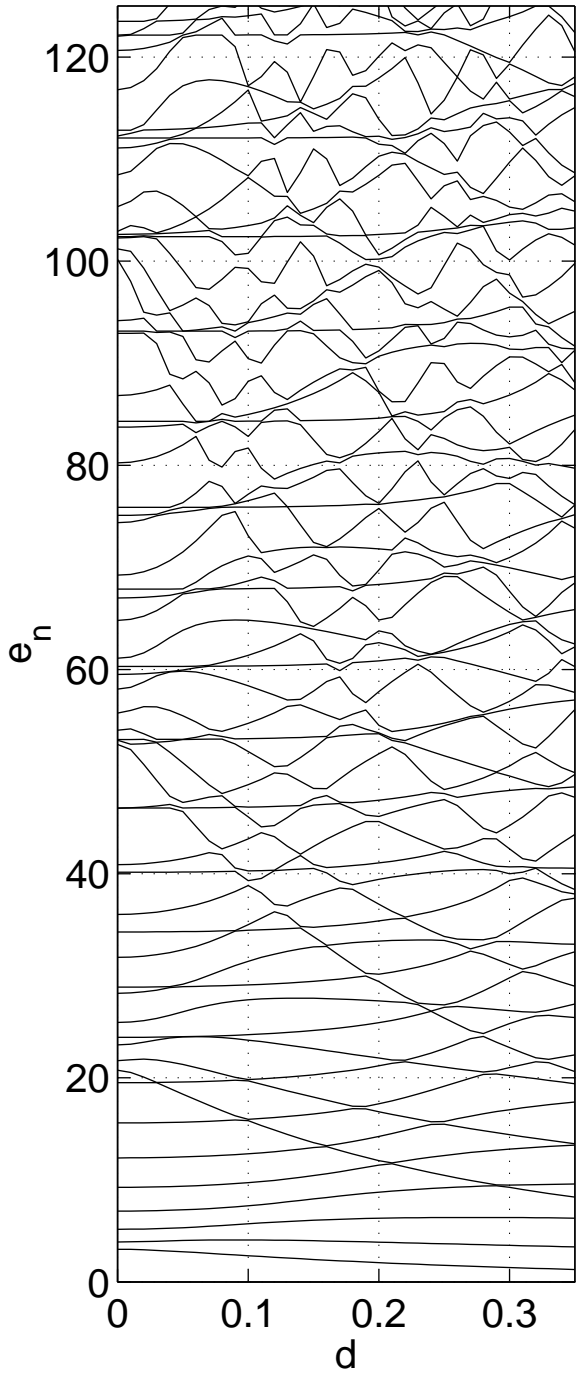
- Fig. 1. The unfolded single-particle spectrum $e_n(d)$, for a circular cavity of unit radius $R = 1$ with a bubble of radius $a = R/2$, as a function of the displacement of the bubble from the center of the cavity d . The even- and odd-parity states are shown separately, in the left and right subplots respectively. The parity is defined with respect to the reflection with respect to the line joining the bubble center to the center of the cavity.

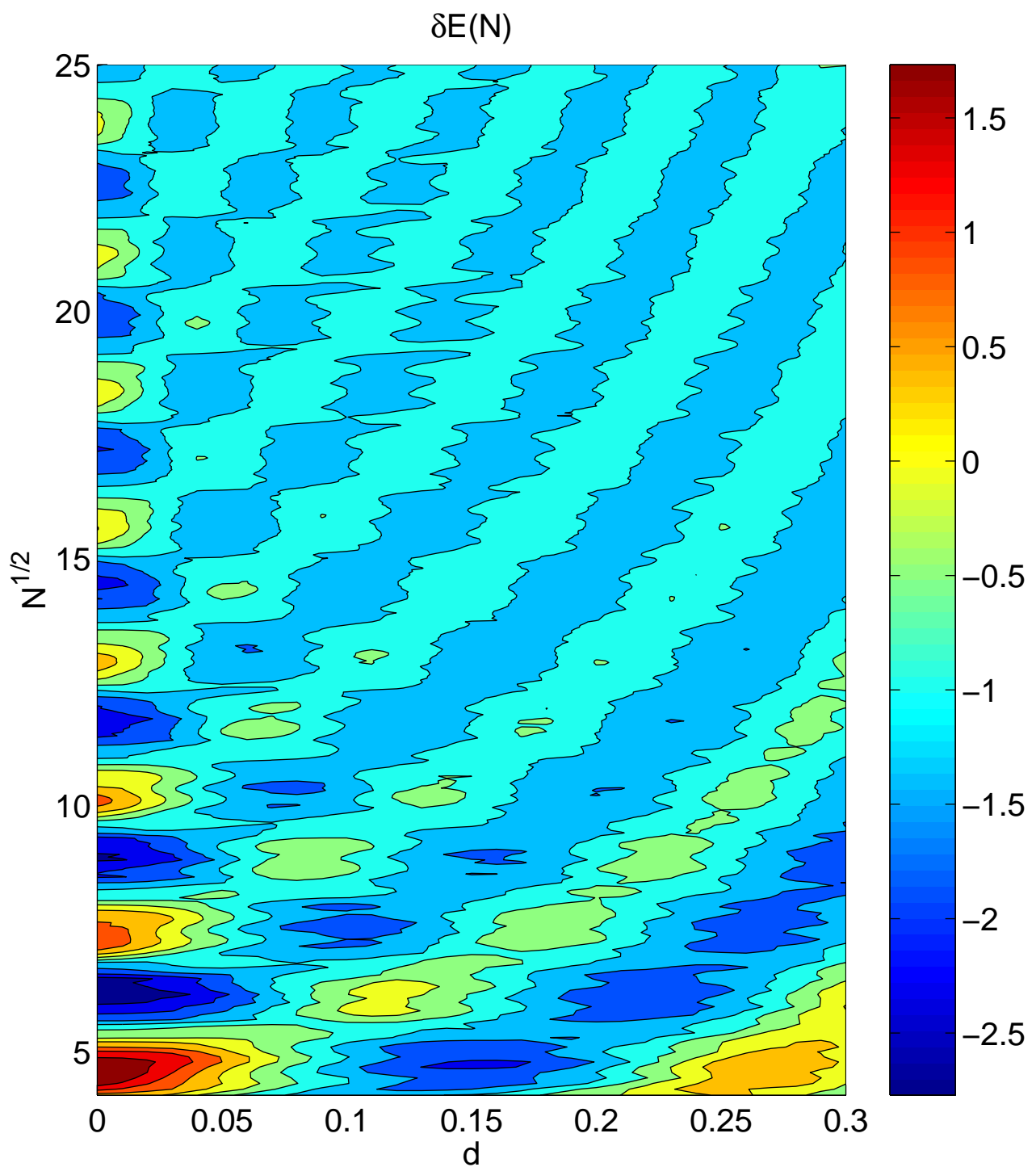
- The contour plot of the shell correction energy $\delta E(N)$, see Eqs. 31, as a function of the $N^{1/2}$ and d . The radius of the system was chosen for each particle number as $R(N) = R_0 N^{1/2} = N^{1/2}$ and in the figure d is the actually the fraction $d/R(N)$. The size of the bubble also scales with the particle number as $a(N) = R(N)/2$.
- Fig. 3. The same as in Fig. 1 but for a smaller bubble with the radius $a = R/5$.
- Fig. 4 The same as in Fig. 2 but for for a smaller bubble with the radius $a(N) = R(N)/5$.
- Fig. 5 The scaled single-particle spectrum $k_n^2(d)d^\alpha$, for two bubbles of unit radius $R = 1$, separated by a distance d . The exponent was determined numerically to be $\alpha \approx 0.425$.

even parity states

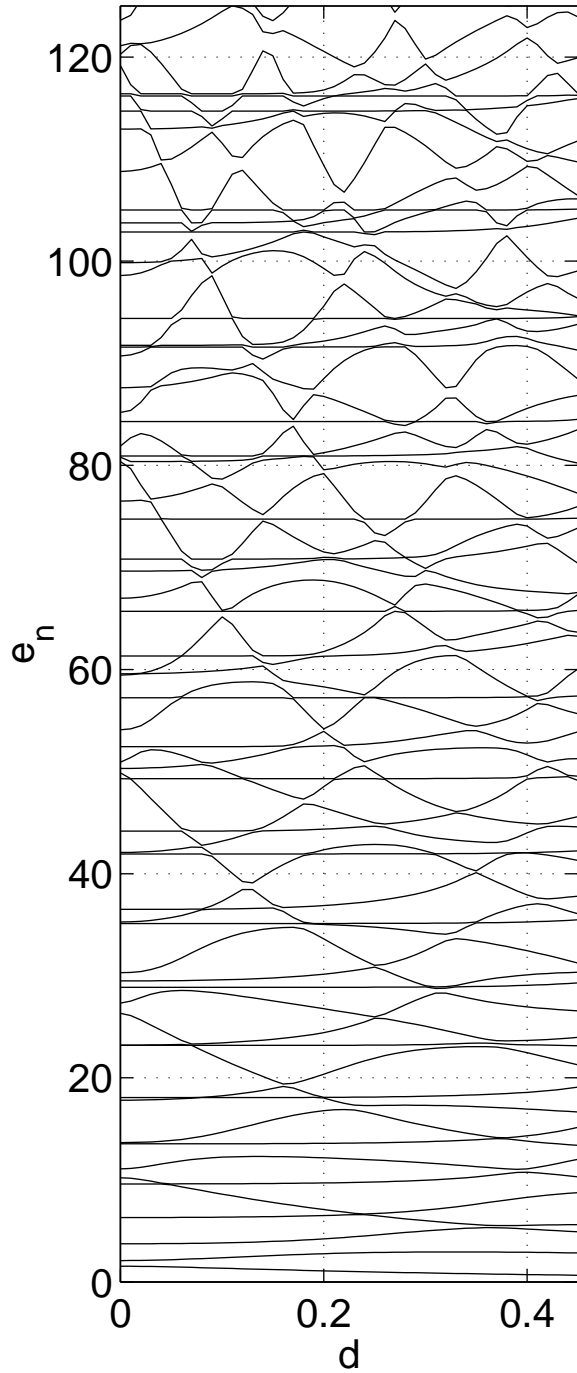


odd parity states





even parity states



odd parity states

